Chemosphere xxx (xxxx) 137075

Contents lists available at ScienceDirect

Chemosphere

journal homepage: www.elsevier.com/locate/chemosphere

Detection and binding interactions of pharmaceutical contaminants using quartz crystal microbalance – Role of adsorbate structure and surface functional group on adsorption

Philomena Oluwatosin Olaniyan, Md-Masuduzzaman Nadim, Mahamud Subir *

Department of Chemistry, Ball State University, Muncie, IN, USA

ARTICLE INFO

Handling Editor: CHANG MIN PARK

Keywords:
Soft interfaces
Emerging contaminants
Self-assembled monolayer
Natural organic matter
Quartz crystal microbalance

ABSTRACT

Hypothesis: Emerging contaminants (ECs) can interact with soft solid/aqueous interfaces of particulate organic matter and microplastics in the aquatic environment but to what extent? It is hypothesized that EC adsorption can be detected using quartz crystal microbalance (QCM), a sensitive gravimetric tool, and their adsorption energetics and uptake capacity can be measured for various substrates of distinct functional group. This in turn reveals the specific vs. nonspecific interactions.

Experiments: QCM has been used to detect and measure the adsorption of selected pharmaceuticals, amlodipine (AMP) and carbamazepine (CBZ), onto butyl, carboxyl, amine, and phenyl functionalized self-assembled monolayers (SAMs), mapping out the hydrophobic effect, H-bonding capability, and $\pi-$ interactions. Adsorption free energy (ΔG_{ads}) and maximum interfacial concentration ($c_{\max}$) for these surfaces are compared. Solvatochromic studies to elucidate the likelihood of H-bonding interactions for CBZ and AMP have been conducted using UV–Vis absorption spectroscopy.

Findings: Amlodipine and carbamazepine adsorb onto butyl/aqueous interface with respective ΔG_{ads} values of -35.8 ± 1.1 and -37.7 ± 0.1 kJ/mol. Nonspecific interaction allows a greater extent of $c_{\max}$ on the hydrophobic/aqueous interface. CBZ is does not bind to the phenyl surface. AMP and CBZ exhibit H-bonding and show proclivity for the amine and carboxyl SAMs. Interfacial chemical environment and adsorbate structural properties play a significant role on EC adsorption.

1. Introduction

Pharmaceutical contaminants are widespread in not only wastewaters but also in surface- and ground-water (Halling-Sørensen et al., 1998; Osenbrück et al., 2007; Barnes et al., 2008; Stuart et al., 2011; Lapworth et al., 2012; Tijani et al., 2016; Bai et al., 2018). They are one of the prime examples of aquatic contaminants of emerging concerns. Pharmaceuticals, both parent compounds and metabolites, are chiefly introduced into the aquatic systems via improper disposal of prescription drugs, human excretion, livestock and veterinary waste, and through agricultural runoff (Osenbrück et al., 2007; Barnes et al., 2008; Stuart et al., 2011; Lapworth et al., 2012). They generally enter the aquatic environment due to inefficient water treatment technology (Lapworth et al., 2012; Fuentes et al., 2020). Throughout the water system, emerging contaminants (ECs) are subject to various interactions with solid substances such as soil, mineral oxides and natural organic matter (NOM). These interactions, such as sorption into the bulk porous solids and adsorption at these solid/aqueous interfaces, can influence the fate and transport of these pollutants (Spain et al., 1983; Klavins and Purmalis, 2010; Wang et al., 2018, 2022a, 2022b; Williams et al., 2020). Within the decade, there has been many chemical research (Schwartz, 2001; Bai et al., 2008; Ruiz et al., 2013; Zhang et al., 2018, 2020, 2022a) geared to the development of materials to remove pharmaceutical and other ECs. Studies involving surface adsorption have been limited. Recent research efforts have demonstrated that ECs can interact with particulate and dissolved NOM and colloidal microplastics (Bai et al., 2008; Ruiz et al., 2013; Wu et al., 2013; Williams et al., 2020). However, it is well-recognized (Keiluweit and Kleber, 2009; Ruiz et al., 2013; Wu et al., 2013; Williams et al., 2020) that additional systematic and fundamental research is needed to better understand the transport, occurrence and fate of ECs. This serves as the primary motivation for the present study, as we seek to elucidate surface binding relationship between pharmaceutical molecular structure and the diverse

* Corresponding author.
E-mail address: msubir@bsu.edu (M. Subir).

https://doi.org/10.1016/j.chemosphere.2022.137075
Received 16 August 2022; Received in revised form 8 October 2022; Accepted 28 October 2022
0045-6535/© 20XX

group of chemical moieties common in NOM and other polymeric particles.

Composed of organic materials, NOM is a complex polymeric structure chiefly composed of humic acids, fulvic acids, and non-humic constituents such as amino acids, proteins, and carbohydrate (Klavins and Purmalis, 2010; Bhatnagar and Sillanpaa, 2017; Chaukura et al., 2018). Carboxylic acids, alkyl chains, alcohols, substituted alkyl and phenyl carbons and amines are some of the common functional groups observed in NOM (Klavins and Purmalis, 2010; Chaudhari et al., 2011; Bhatnagar and Sillanpaa, 2017; Chaukura et al., 2018; Ariga et al., 2019). The same is true of the surface composition of microplastics (Wilkinson et al., 2017; Williams et al., 2020; Zhang et al., 2022b). Moreover, a variety of functional groups are present in organic contaminants. As a result, in addition to chemisorption, wide ranging intermolecular interactions, such as electrostatic, hydrogen bonding, hydrophobic, and π-interactions, are likely. The latter can include π-π, π-cation, or π-anion modes of binding in the presence of aromatic rings (Tsou et al., 2002; Keiluweit and Kleber, 2009; Wu et al., 2013). Since the surface functionalities of particulate NOMs and microplastics can be a mixture of the various functional groups, a fundamental question that arises is: do pharmaceutical contaminants exhibit a preferential adsorption to any of these chemical moieties? A systematic study is needed to elucidate the type of interactions that govern the adsorption of trace quantities of emerging contaminants to these surfaces from aqueous solution.

To this end, we have developed a method to study specific surface interactions based on a gravimetric technique using a quartz crystal microbalance (QCM). Our approach has been to fabricate model surfaces of specific chemical identity onto which adsorption of selected pharmaceutical compounds, carbamazepine (CBZ) and amlodipine (AMP), is monitored. CBZ and AMP have been chosen due to their prevalent detection in the aquatic environment as well as for their distinct chemical structures and properties. To generate the surface of interest, the method of self-assembled monolayer (SAM) formation (Nagaoka et al., 1999; O'Sullivan and Guilbault, 1999; Fung and Wong, 2001; Chaki and Vijayamohanan, 2002) has been employed. SAMs of the following functional groups, carboxyl, amine, phenyl, and butyl, with which ECs can interact, have been prepared. These SAMs serve as models for NOM and microplastic surfaces with known functional groups. Our objective has been to generate adsorption isotherms for CBZ and AMP adsorption onto these SAM/aqueous interfaces. The hypothesis is that these compounds are likely to exhibit different extent of proclivity for these interfaces, which will manifest in the respective Gibbs free energy of adsorption (ΔG_{ads}). Comparing the ΔG_{ads} values thus allow the determination of the relative favorability of binding to these solid/aqueous interfaces and moreover sheds light on the type of interactions responsible for the adsorption process. For instance, ΔG_{ads} for the butyl/aqueous interface would reflect the hydrophobic interactions of these ECs, whereas adsorption of these compounds on the carboxyl and amine functionalized SAM would map out H-bonding in addition to hydrophobic interactions. If specific interaction drives the adsorption process, the surface coverage on these substrates is also likely to vary. Addressing the question of whether pharmaceutical contaminants exhibit preferential adsorption is important in elucidating their fate and transport in the aquatic medium. Moreover, knowledge of EC-surface specific interactions is valuable in developing adsorption-based pollution remediation technology for contaminants of emerging concern (Akhtar et al., 2016; Williams et al., 2016; Bhatnagar and Sillanpaa, 2017).

In addition to the QCM-based adsorption studies, we also performed solvatochromic UV–Vis absorption measurements on CBZ and AMP. Molecular electronic transitions can depend on intermolecular interactions as such that the interaction with the surrounding solvent molecules lead to a shift, either bathochromic (red-shift) or hypsochromic (blue-shift), in the absorbance band of the solute molecule (Nunes et al., 2014; Bani-Yaseen et al., 2019; Yang et al., 2019). In particular, the spectral shift in binary mixtures of hydrogen-bond accepting and donating solvents, such as 1, 4-dioxane:water mixture, can be used to evaluate the possibility of H-bonding (Bani-Yaseen et al., 2019). This has been the basis to assess the likelihood of CBZ and AMP in participating in H-bonding, which in turn helps understand their interfacial interaction with model particulate NOMs and microplastics. Together with the solvatochromic and QCM-based isotherm data, we have thus achieved the goal of deciphering the type of binding interactions AMP and CBZ can exhibit. We show that the QCM method can be used to detect and probe surface interaction of ECs from aqueous solution. QCM has often been applied to detect adsorption of volatile organic molecules from gas phase, and macro- and bio-molecules from aqueous and nonaqueous solvents (Caruso et al., 1996; Vashist and Vashist, 2011; Tonda-Turo et al., 2018; Roshani et al., 2022). To the best of our knowledge, this is the first demonstration of its utility in probing adsorption of pharmaceutical contaminants from an aquatic medium. Furthermore, we have quantified the adsorption free energy for each of these pharmaceutical-surface interactions. Comparison of these values reveal intriguing adsorption behavior for these contaminants and the type of interaction that dominates. Their affinity for these surfaces, or lack thereof, are discussed in terms of possible H-bonding, hydrophobic, Coulombic, and π-interactions. Thus, this work not only has practical significance in environmental remediation, and fate and transport of the selected pharmaceutical ECs, but also provide fundamental insights into the relationship between interfacial chemical composition and molecular structure of the organic pollutant.

2. Experimental

Chemicals and Materials – All the pharmaceuticals and thiol compounds were purchased from Sigma-Aldrich. These include carbamazepine (Prod. No. 94496) and amlodipine besylate (Prod. No. PHR1185), phenylethyl mercaptan (Prod. No. W389404, a.k.a. 2-phenylethanethiol, PET), 1-butanethiol (BET, Prod. No. 112925), cysteamine hydrochloride (Prod. No. M6500, a.k.a. 2-aminoethanethiol, AET) and 3-mercaptopropionic acid (MPA, Prod. No. M5801). Fig. 1a shows the molecular structures of the thiol compounds used to prepare self-assembled monolayers (SAMs). Neat solvents of spectroscopic grades were ordered from Sigma-Aldrich and Fischer Scientific. All the chemicals were used as received. Aqueous solutions were prepared using Millipore water (Milli-Q, 18.2 $M\Omega/cm$). The ionic strength of all the solutions is thus determined by the concentration of the charged analytes, and is in the order of $_{10}{}^{-6}$ M. Electrolytes were not added to adjust the ionic strength. The pH of all the solutions prepared was 6.9 ca. All glassware used in sample preparation were soaked in aqua regia (3:1 M ratio of HCl:HNO_3) and rinsed vigorously with DI water. Millipore water was used for the final rinse before solution preparation. Disposable sterile polystyrene pipets and borosilicate glass pipets (Fisher Scientific) were used to prepare solutions in aqueous and organic solvents, respectively.

UV–Vis Solvatochromic Study – Solvatochromic behavior of the target pharmaceuticals was studied using UV–Vis spectroscopy (Shimadzu UV-1800). Two distinct experiments were conducted: (1) the absorption spectra of AMP and CBZ in ten (10) neat solvents of varying polarities. They include polar protic (water, methanol, ethanol, and isopropanol), polar aprotic (acetonitrile, ethyl acetate, acetone, and tetrahydrofuran) and non-polar (chloroform and 1,4-dioxane) solvents. (2) the absorption spectra of AMP and CBZ in a binary mixture of water and 1, 4 – dioxane of varying proportion of the solvents. For the binary mixture study, to assess the possibility of hydrogen bonding, 1,4-dioxane: water mixtures by volume were prepared within the range of 0–100% of dioxane. The absorption spectra were collected within the range of 190 nm and 700 nm. The 1,4-dioxane:water mixture is commonly used because the two solvents are miscible and are similar in terms of their viscosity and density (Casassas et al., 1992; Bani-Yaseen et al., 2019).

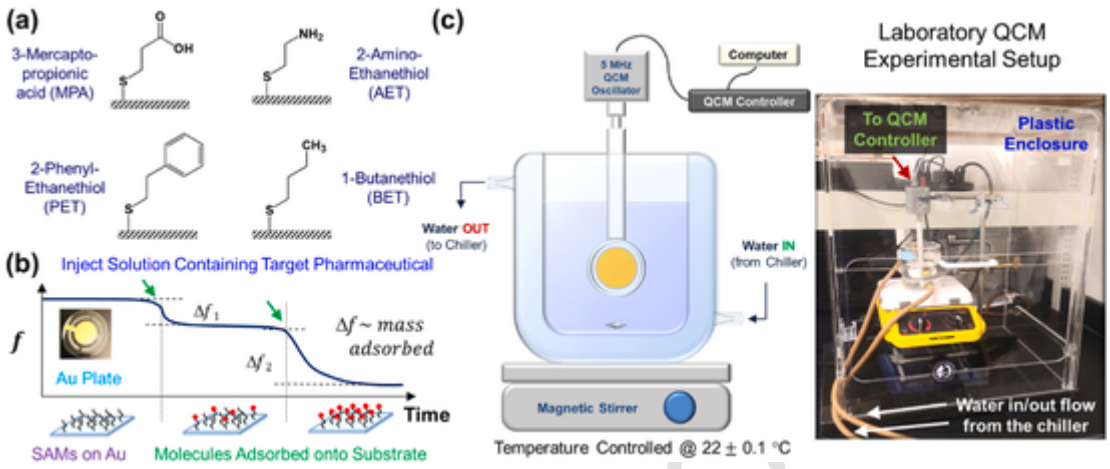

Fig. 1. (a) Molecular structures of the thiol compounds used to prepare SAMs. (b) a schematic describing the working principle of measuring the QCM frequency as a function of time and the changes associated with mass uptake. (c) A cartoon and a photograph showing the QCM experimental setup, emphasizing the importance of good temperature control and enclosure to minimize drafts.

Quartz Crystal Microbalance – The 5 MHz QCM unit (QCM200) has been purchased from Stanford Research System (SRS). Using a 10 s gate the measurement resolution was 0.01 Hz. The experiments were conducted using a 1-inch diameter AT-cut quartz crystal wafer with gold (Au) coated circular electrode (also purchased from SRS). The sensitivity factor (C_f) of the crystal is 56.6 $Hz\ \mu g^{-1} cm^2$ at room temperature and the surface area of the gold plate exposed to the solution is $\sim 1.37\ cm^2$. However, the displacement or the active area of oscillation is restricted to $\sim 0.4\ cm^2$. (2018) The data was collected using a LabView program. In generating an adsorption isotherm – a plot of the concentration of the solute adsorbed vs. its equilibrium concentration remaining in the solution – the typical experiment entailed recording the frequency as a function of time, as shown in Fig. 1b. The change in the frequency, upon introducing the target compound (either the thiol compounds onto the bare gold plate or pharmaceuticals at the SAM/aqueous interface), is first converted to mass uptake (Δm) using the Sauerbrey equation (Eq. (1)). The mass uptake is used to calculate the concentration of the solute adsorbed. An important criterion for the applicability of Sauerbrey equation is that the adsorbed film is thin, uniform, and rigid (Vogt et al., 2004, 2018; Easley et al., 2022). For this reason, we have opted for SAMs with shorter carbon chain.

$$\Delta f = -C_f \Delta m \qquad 1$$

Fig. 1c shows a diagram of the experimental approach and a photograph of the setup. A glass jacketed beaker was filled with a 150 mL of the desired solvent. Hexane was used for the thiolation of hydrophobic PET and BET, and water for the remaining thiols (MPA and AET) and the pharmaceuticals. In a typical experiment, the QCM electrode is submerged in the liquid, the capacitance nullified, and the frequency monitored for stability. Once the stability is reached, the first injection is made and a frequency drop is observed. Subsequent injection is made after an equilibrium, as ascertained from constant frequency reading, is reached. The total amount of volume introduced using a micro syringe was not more than 10 mL in all cases. The injected volume ranged from 0.1 mL to 0.5 mL. Volume change has been considered in calculating the final concentration of the target compound. Sufficient time was provided in between injections for equilibrium between the surface and the solution to be reached. In all cases, this time is at least 20 min until a plateau in the kinetic profile (frequency vs. time) is reached. It is important to note that maintaining a constant temperature is essential for accurate measurements, particularly in aqueous solution due to the large thermal coefficient of viscosity of water. The temperature of the solution was kept constant at 22 ± 0.1°C using a chiller and a plastic enclosure was used to minimize drafts. The solution was stirred constantly and the data was collected at a 10 s interval.

2.1. Preparation of SAMs

The method of creating SAMs via chemisorption of organothiols from solution is well established and has been exploited before (Akiba and Fujihira; Love et al., 2005; Vashist and Vashist, 2011). Our approach has been to generate a monolayer through step-by-step injections and by monitoring its progress using QCM. This method has been inspired by the work of Karpovich and Blanchard (Karpovich and Blanchard, 1994, 1995), but modified to accommodate short-chain organothiols. An advantage of this protocol of adsorption from solution, as opposed to generation of SAMs using concentrated thiols, is that it allows the visualization of the surface saturation. Moreover, formations of multilayer and inhomogeneous patches are avoided, when diluted solutions are used.

Molecular Modeling – To obtain information about the molecular dimensions, Avogadro, an open-source molecular builder and visualization tool (Version 1.XX), has been used (Hanwell et al., 2012). MMFF94 molecular mechanics and force fields, which is particularly good with organic compounds, have been employed to optimize the geometry of the molecules. Optimization, which minimizes the energy, was performed using the Steepest Descent algorithm without fixing any atoms. Once optimized, the dimensions (the length and the width) of the molecule was measured using the built-in measure tool. The molecular area was estimated by the circular area (πr^2) the molecule occupies on the surface.

3. Results and discussion

The experimental results of this work are presented in the following order: UV–Vis solvatochroomic data of CBZ and AMP, followed by results pertinent to the thiolation of Au quartz plates, and lastly, data corresponding to the CBZ and AMP adsorption onto the SAMs of different functional groups. The first section will provide insights into the possible interactions these contaminants can have, and will facilitate the discussion in the latter section which will present the effect of surface functional groups on their adsorption behavior.

3.1. Insights from solvatochromic studies

We begin the discussion by exploring few of the structural features of CBZ and AMP and presenting their UV–Vis solvatochromic properties. CBZ is a rigid molecule with zero rotatable bond counts (RBC);

whereas, RBC of AMP is ten. Experimentally, we found the solubility of amlodipine besylate and CBZ in neat water to be approximately 130 μM and 75 μM, respectively. AMP is a positively charged molecule whereas CBZ is neutral. Fig. 2 shows both the Kekulé and 3D structures of these molecules. It is clear that there are more polar groups in AMP than the CBZ. The polar surface area of CBZ is 46.3 $Å^2$ and that of AMP is 99.9 $Å^2$. Additionally, AMP has five hydrogen-acceptor count and two hydrogen-donor count; whereas, CBZ has one each. Thus, both AMP and CBZ are likely to exhibit H-bonding, with AMP having the greater likelihood.

To deduce if CBZ and AMP participate in H-bonding, we performed solvatochromic studies based on UV–Vis absorbance spectroscopy. Fig. S1 (top panel) in the Supplementary Material File shows the normalized absorbance spectra of these compounds in various solvents of different polarity. AMP shows a red shift with increasing solvent polarity and CBZ, a slight blue shift. Such muted variation with increasing solvent polarity suggests that CBZ prefers nonpolar environment. These spectral shifts can be visualized (Fig. S1, bottom panel) better as a plot of transition wavenumber vs. solvent orientation polarizability ($\Delta f(\varepsilon, n)$). The $\Delta f(\varepsilon, n)$, which is a function of the dielectric constant (ε) and refractive index (n) of the solvent, describes the general solvent effect. It accounts for the reorientation of the solvent molecules; thus, a nonlinearity in the spectral shift as a function of $\Delta f(\varepsilon, n)$ generally indicates that specific solvent effects are involved. Our results show a poor linear correlation ($R = -0.40$) between the transition wavenumber and polarizability for AMP and a weak to moderate correlation ($R = 0.74$) for CBZ. This is a tell-tale sign that these compounds are exhibiting interactions that goes beyond the van der Waals type interaction. The solvent-solute interaction is not solely explained by the polarity of the solvent. Additional interactions, such as H-bonding, are possible.

To further verify the tendencies of AMP and CBZ to form hydrogen bonding, solvatochromic behavior in miscible binary mixtures of water and 1,4-dioxane, a H-bond acceptor, has been measured. Fig. 2 displays the shift in spectral transition of AMP (a) and CBZ (b) as the water content is varied. The key idea is that we see a strong linear correlation for AMP ($R = -0.92$) and a fair level of correlation for CBZ ($R = 0.76$). This result is consistent with the number of H-bond donor and acceptor counts for these molecules. AMP has the greatest possibility of forming H-bonding as is evident by the strong correlation; however, this possibility is limited for CBZ. While solvent-solute interaction, as assessed based on solvatochromic studies, provides insights into the type of interactions these pharmaceutical contaminants can have, it does not necessarily explain whether interfacial adsorption of these compounds will be favorable with substrates containing H-bond donating/accepting functional groups. Interfacial interactions entail additional factors. For instance, conformational and orientation changes in the adsorbate are often required before sufficient interaction can take place, creating an energetic barrier to the adsorption process. Moreover, entropic cost associated with the dissociation of the target compound from its solvent environment and the displacement of solvent molecules from the surface also must occur in the exchange process of adsorption in contact with the aqueous solution. This necessitates performing adsorption experiments, which we turn to next.

3.2. Analysis of SAMs

Both enthalpic and entropic contributions, which manifest in the ΔG_{ads}, dictate the overall favorability of an adsorption process. Measuring ΔG_{ads} of pharmaceutical contaminants thus has been the ultimate goal of this work. However, as discussed in the Introduction section, en-

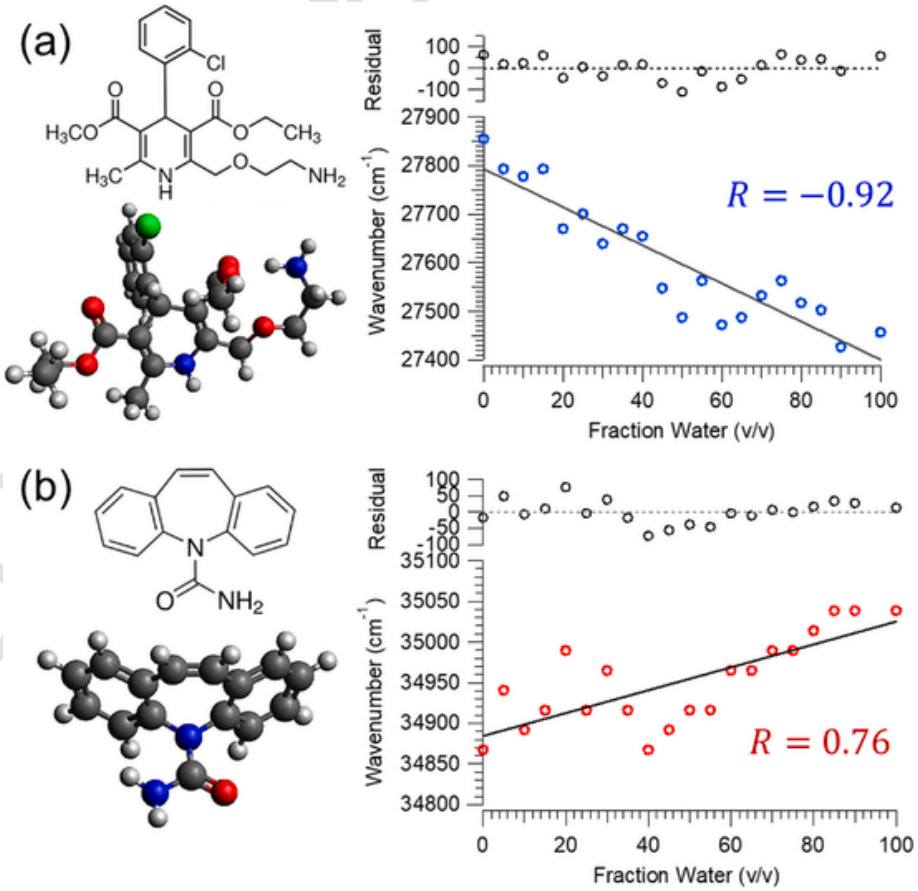

Fig. 2. Molecular structures of AMP (top panel) and CBZ (bottom panel). Transition wavenumber of (a) AMP and (b) CBZ, obtained from UV–Vis absorbance spectroscopy, as a function water fraction by volume in a binary mixture of water and 1,4-dioxane.

vironmental interfaces are complex, i.e., can contain a diverse class of chemical functional groups. To deduce specific surface interaction and the effect of functional groups it was necessary to fabricate SAMs of specific chemical group. Here we discuss the results of SAM preparation based on the QCM method. Representative adsorption isotherms for BET, PET, MPA, and AET are shown in Fig. 3. Fitting of the adsorption isotherms also permit quantitative analysis of the SAM formation. Data pertinent to control experiments, in which aliquot of the solvent (without the target thiol) is injected, are shown in the Supplementary Document (Fig. S2). They clearly show that the frequency remains unchanged, within the experimental uncertainty of ± 0.5 Hz.

Fig. 3 reveals that the adsorption isotherms of SAMs follow a Langmuirian profile. The y-axis is the concentration of the target thiol compound adsorbed calculated from the frequency change using Eq. (1). The mass change was converted to concentration using the known molar mass of the adsorbates. By fitting the data using the Langmuir isotherm model (Eq. (2)), we thus obtain ΔG_{ads} of thiolation and the maximum surface concentration, $c_{\max}$.

$$c_{ads} = c_{\max} \frac{K_{ads} \frac{c}{c_o}}{K_{ads} \frac{c}{c_o} + 1} \qquad 2$$

In this equation, K_{ads} is the adsorption equilibrium constant, c_{ads} and c are the concentrations of the target compound adsorbed at the surface and the remaining in solution, respectively. The concentration of the solvent, c_o, is a fixed parameter and is 55.5 for water and 7.60 for hexane. The Gibbs free energy of adsorption is obtained using $\Delta G_{ads} = -RTlnK_{ads}$. Multiple trials of the adsorption isotherm measurements have been conducted (Figs. S4–S7). The residuals of the fit are shown and the Chi-Square (χ^2), which is the sum of the residuals are reported within each figure. The minimized χ^2 values are small, ranging in the order of 10^{-21} to 10^{-19}. For a given experimental data, fitting with other isotherm models, such as the Freundlich model, yield higher χ^2 value, suggesting the Langmuir model to be the better description of the experimental data. The average values of ΔG_{ads} and $c_{\max}$, along with the corresponding standard errors, are presented in Table 1. The individual errors in each fitting parameter are smaller than the standard errors tabulated. The reported standard error thus represents the true uncertainty in these measurements.

As expected, the formation of SAM from these organothiol compounds from the respective solution are spontaneous as indicated by the negative ΔG_{ads} values. The Gibbs free adsorption of octadecanethiol from hexane has been reported to be −23.4 ± 1.7 kJ/mol (Karpovich and Blanchard, 1995). For butylthiol, we find it to be −35.1 ± 1.4 kJ/mol, suggesting that its adsorption is thermodynamically more favorable than that of octadecanethiol. This is reasonable because longer chain thiol would be more favorably solvated in the nonpolar hexane than that of the thiol compounds with shorter alkyl chain such as BET. The method of SAM preparation adapted here also provides an insight into the interfacial coverage of these thiol compounds on the gold surface. Converting the fit parameter $c_{\max}$ to area per molecule we find PET to occupy the largest area (Table 1). Considering the molecular dimension of these molecules (Fig. 3), a molecular area of 60 ± 15 for PET indicates that the phenyl group is lying flat on the gold. Whereas the other compounds are likely oriented upright and slightly tilted. The implication is that the subsequent adsorption of pharmaceutical compound will exhibit interaction with the phenyl ring.

3.3. Adsorption of pharmaceuticals onto SAMs

To assess specific interactions, we have performed adsorption studies of AMP and CBZ onto these functionalized SAMs. The results are shown in Fig. 4. The control experiment for this study involved intro-

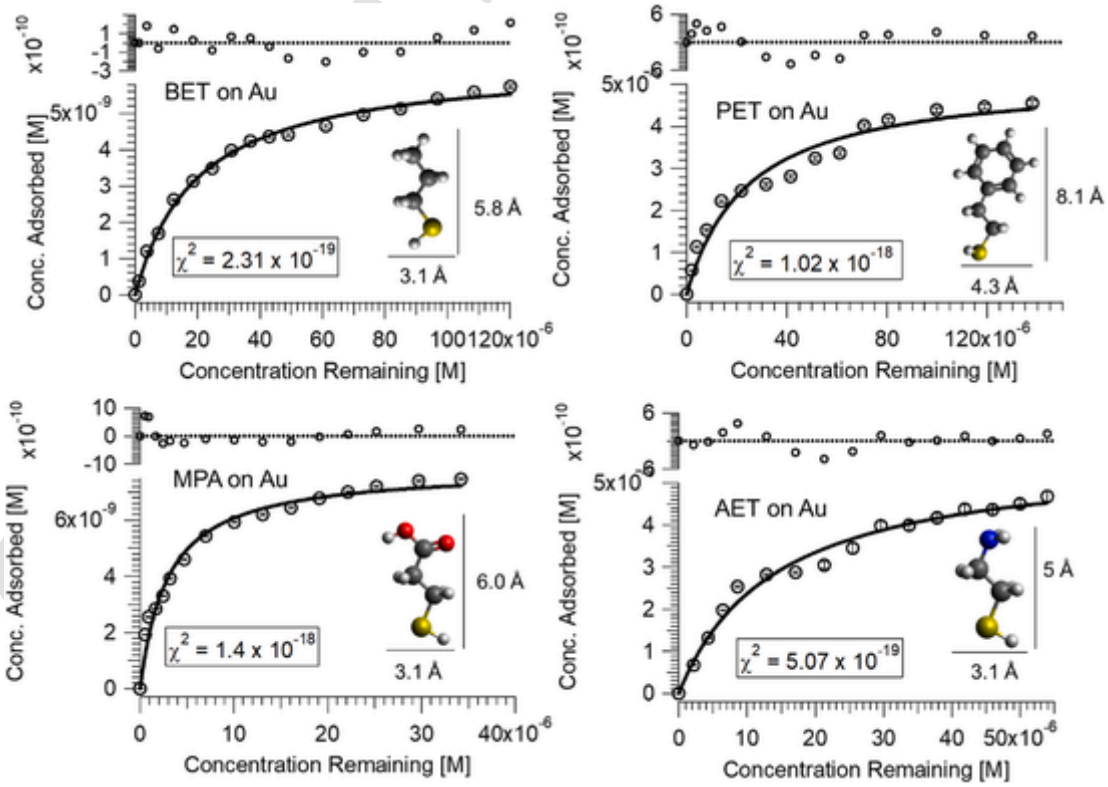

Fig. 3. Representative thiolation isotherms showing the adsorption of the target thiol compound on gold-quartz plate. The residuals of the fit are shown on the top panel. The minimized χ^2 values are also shown. The insets show the molecular dimensions of the thiol compounds used. Additional trials for each of the thiolation are shown in the Supplementary Material File (Figs. S4–S7). (For interpretation of the references to colour in this figure legend, the reader is referred to the Web version of this article.)

Table 1
Thermodynamic parameters of adsorption of organothiol compounds onto gold surface.

Functionalized Surface (Solvent)	c_{max} (nM)	Molecular Area ($Å^2/molecule$)	ΔG_{ads} (kJ/mol)	No. of Trials
BET (Hexane)	6.0 ± 1.3	28 ± 6	−35.1 ± 1.4	5
MPA (Water)	7.6 ± 1.8	24 ± 5	−43.1 ± 1.3	5
PET (Hexane)	3.0 ± 0.7	60 ± 15	−33.3 ± 1.0	5
Amine (Water)	6.1 ± 1.4	26 ± 5	−39.0 ± 1.1	4

ducing the target compound into the aqueous solution in contact with bare gold plate without the SAMs. The QCM response is within experimental uncertainty (Fig. S3). That is, within the experimental uncertainty, adsorption of CBZ and AMP on neat gold/aqueous interface is either negligible or does not occur. Accordingly, the adsorption isotherms shown in Fig. 4 reflect the uptake of these target compounds solely onto the SAMs of specified functional group. The average adsorption Gibbs free energy and maximum surface concentration obtained for multiple trials are tabulated in Table 2. It is clear that surface functional group does influence not only the spontaneity of the adsorption process but also the overall surface coverage.

As dictated by the ΔG_{ads} values, we see that the proclivity for the different surfaces vary for each of the compound. Adsorption of both AMP and CBZ onto the hydrophobic butyl/aqueous interface is favorable, exhibiting similar ΔG_{ads}. This is reasonable because adsorption on the alkyl surface represent a non-specific interaction. Adsorption onto this alkyl hydrocarbon model surface is predominantly due to hydrophobic effect, which entails both enthalpic and entropic contributions. That is, it represents van der Waals type interaction and the change in entropy that occurs due to the rearrangement of water molecules as the solute detach from the solvent (de Jesus and Yin, 2017). In a recent study (Dalla Pozza et al., 2022), it has been shown that both CBZ and AMP exhibit affinity toward the air/aqueous interface, with the ΔG_{ads} found to be —30.9 ± 0.3 kJ/mol and —32.3 ± 0.9 kJ/mol, respectively. The air/water interface is considered to be hydrophobic and repartitioning of the solvent energy drives the adsorption (van Oss et al., 2005; McCaffrey et al., 2017). In the case of adsorption to the alkyl/aqueous interface, it is revealed that the adsorption is more spontaneous, likely due to the favorable enthalpy change arising from the van der Waals interaction. Our results also suggest CBZ adsorption is slightly more favorable than that of AMP. If we assume, both CBZ and AMP to exhibit the same extent of van der Waals interaction with butyl surface, the difference in their ΔG_{ads} values can be attributed to the entropic hydrophobic effect. Since CBZ is a rigid molecule, there is an entropic cost for water molecules to solvate CBZ in the bulk solution. CBZ adsorption on the surface, or its expulsion from the aqueous solution, therefore leads to an increased disorder in the solution phase water molecules, providing the extra driving force that manifests in the more negative ΔG_{ads} value.

Comparing the AMP and CBZ adsorption behavior onto the butyl hydrophobic/aqueous interface with that of SAMs containing the other functional groups, it is evident that the interfacial chemical moiety does influence the adsorption affinity of these emerging contaminants. Moreover, the surface coverage of these adsorbates varies with the composition of SAM/aqueous interface. This is visualized in the plot (Fig. 5) of the relative interfacial coverage of the target pharmaceutical for each type of SAM studied. The ratio in this plot is calculated by dividing the maximum surface coverage of the pharmaceutical on a particular SAM/aqueous interface by that of the corresponding surface coverage of SAM on the gold plate. This ratio is an intensive property that signifies the fraction of contaminant for a given SAM. For the butyl (BET) surface, this ratio is the highest and the same for both CBZ and AMP. This is expected because these compounds exhibit nonspecific interaction at the butyl/aqueous interface. Proper alignment or reorientation at the surface is not necessary to bind to this hydrophobic SAM, resulting in a broader surface coverage. Other surfaces show diminished interfacial coverage ratio, which indicates that specific interactions and proper alignment with specific functional group dictates adsorption.

An intriguing finding is that CBZ does not adsorb onto the phenyl functionalized SAM. This we attribute to possible repulsive interactions between the π electrons of the phenyl substrate and that of the CBZ. As assessed from the surface coverage and molecular dimension of the thiolated compounds (Table 1), the phenyl ring is likely oriented flat on the surface. A surface interaction between the rigid CBZ molecule with the phenyl group would thus predominantly entail CBZ molecule lying flat, yielding a face-to-face or sandwich-like interaction. However, this alignment would lead to a repulsion between the π electron clouds which can outweigh the hydrophobic interaction (Cabaleiro-Lago and Rodríguez-Otero, 2018; Molčanov and Kojić-Prodić, 2019). The outcome is the limited or no adsorption as observed. The rigidity of the CBZ molecule is also likely to prevent its realignment for a more favorable surface interaction with the phenyl functionalized SAM. On the other hand, AMP, with a greater degrees of rotatable bond count, has the flexibility to reorient itself for a favorable interaction with the phenyl group. It is likely that the positively charged amine group on AMP interacts with the electron rich phenyl. Of all the SAM/aqueous interfaces studied, our results indeed show that AMP adsorption on PET has the highest $-\Delta G_{ads}$ value (Table 2). This is consistent with the fact that bonding strengths of cation-π interaction can exceed or be competitive with that of the H-bonding interaction (Keiluweit and Kleber, 2009; Dougherty, 2013). However, strong affinity does not necessarily translate to highest interfacial population. It is noted that surface coverage of AMP on phenyl functionalized SAM is much less compared to

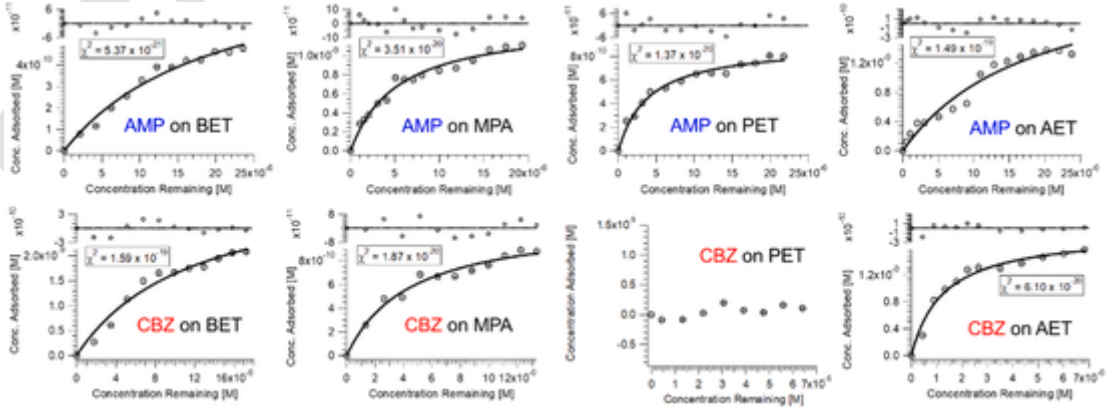

Fig. 4. Representative isotherms for AMP (top panel) and CBZ (bottom panel) adsorption onto SAMs of distinct chemical composition. The residuals of the fit are shown on the top panel. The minimized χ^2 values are also shown. Additional trials are shown in the Supplementary Material File (Figs. S8–S15).

Table 2
Thermodynamic parameters of adsorption organothiol compounds onto gold surface.

SAM	Amlodipine			Carbamazepine		
	c_{max} (nM)	ΔG_{ads} (kJ/mol)	No. of Trials	c_{max} (nM)	ΔG_{ads} (kJ/mol)	No. of Trials
BET	4.2 ± 1.1	−35.8 ± 1.1	6	4.1 ± 0.50)	−37.7 ± 0.1	4
MPA	1.6 ± 0.3	−38.5 ± 0.7	3	1.8 ± 0.3	−37.7 ± 1.2	4
PET	0.4 ± 0.1	−40.1 ± 1.6	4	No Adsorption		3
AET	2.5 ± 1.1	−36.8 ± 0.5	4	1.8 ± 0.4	−41.3 ± 2.1	4

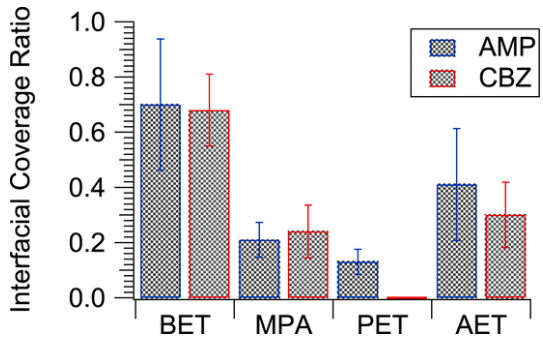

Fig. 5. Relative surface coverage of AMP (blue) and CBZ (red), represented as a ratio of c_{max} of the target pharmaceutical to c_{max} of the SAM, onto different SAM/aqueous interfaces. (For interpretation of the references to colour in this figure legend, the reader is referred to the Web version of this article.)

that of the other surfaces (Table 2 and Fig. 5), as is anticipated in the case of specific cation-π interaction.

The adsorption behavior of CBZ and AMP on the phenyl surface highlights the importance of surface composition in dictating molecular adsorption. While it is apparent that these two structurally and electrostatically different pharmaceutical contaminants can and do adsorb via hydrophobic interactions, distinct interfacial chemical moieties can hinder their uptake. Our QCM based adsorption studies also show that adsorption of both CBZ and AMP onto carboxyl and amine functionalized SAM is favorable. Given the interfacial coverage ratio for these surfaces is less than that of the butyl/aqueous interface, it is surmised that in addition to van der Waals interaction, specific interactions, such as H-bonding, is likely responsible for the overall driving force for the adsorption. The solvatochormic study presented (Fig. 2) does indicate that both CBZ and AMP are susceptible to H-bonding. However, direct evidence, based on interfacial selective vibrational spectroscopy is warranted to obtain a molecular level understanding of the specific interaction. For instance, vibrational sum frequency generation has been powerful in identifying chemical species at various soft interfaces (Rao et al., 2009; Hosseinpour et al., 2012; Jubb et al., 2012; Johnson and Baldelli, 2014; Chase et al., 2015; Ho et al., 2016; Subir and Rao, 2021). At this juncture, it is important to emphasize that the adsorption favorability for the surfaces where specific interactions are possible, is either comparable or slightly greater than that of the hydrophobic butyl/aqueous interface. An increase in the $-\Delta G_{ads}$ is anticipated due to the enthalpic contribution from specific interactions but our data suggests that the effect of specific functional group on the energetics of adsorption is miniscule. What is significantly affected by the interfacial chemical composition however is the amount of the target contaminant adsorbed.

4. Conclusion

In this original study, we have demonstrated that quartz crystal microbalance gravimetric technology, in conjunction with thiolated self-assembled monolayer preparation, can be used to detect the adsorption of trace level of emerging pharmaceutical contaminants from an aquatic medium. This is a major achievement since quartz crystal microbalance has been predominantly used for investigating adsorption from gas phase or organic solvents, and of macromolecules from aqueous solutions. Furthermore, the focus of this study has been to systematically identify the effect of surface functional group on organic contaminant adsorption. By fabricating self-assembled monolayer composed of distinct functionalities we have mapped out the influence of specific chemical groups anchored at a given substrate on the adsorption of selected pharmaceutical compounds known to be of emerging concern. Our results provide fundamental insights into the adsorption behavior of amlodipine, a charged species, and carbamazepine, a rigid neutral molecule, onto various soft interfaces. It is shown that both amlodipine and carbamazepine are subject to hydrophobic effect and can accumulate at the polymeric alkyl/aqueous interfaces. They also show proclivity for amine and carboxyl functionalized planar substrate/aqueous interfaces. Solvatochromic studies support the hypothesis that H-bonding plays a role for the adsorption onto these surfaces. An intriguing finding revealed in our data is that carbamazepine does not show proclivity for the phenyl/aqueous interface. Based on the surface coverage and adsorbate structural properties, we have deduced $\pi - \pi$ repulsion is responsible for the lack of carbamazepine adsorption on the planar phenyl surface. Amlodipine, on the other hand, shows a strong affinity for the phenyl substrate likely due to cation $-\pi$ interaction.

The fundamental insights obtained in this study are valuable in deciphering the fate and transport of emerging organic micropollutants. Many particulate matter (e.g. natural organic matter and microplastics) in the aquatic environment provide sufficient surface area for molecules to adsorb. These particle/aqueous soft interfaces are complex and exhibit a diverse surface chemistry. Often octanol-water partition coefficients are used to assess their distribution in the aquatic environment but as this study has shown chemical identity of the substrate and structural properties of the adsorbate can influence not only the driving force for the surface accumulation but also the interfacial coverage. For instance, while hydrophobic interfaces can accommodate the highest surface coverage due to nonspecific interactions, certain functional groups on the colloidal surface can limit interfacial adsorption. These physical insights into the interfacial interaction would not have been possible without the systematic approach of quartz crystal microbalance-based detection and studying the adsorption on specific self-assembled monolayer surfaces. Our study provides a macroscopic understanding of these interfacial processes and motivates a deeper molecular level understanding using interfacial selective spectroscopic techniques.

Author contributions statement

Philomena Olaniyan: Data curation, Formal analysis, Investigation, Methodology, Project administration, Validation; **Md-Masuduzzaman Nadim:** Data curation, Formal analysis, Investigation, Validation; **Mahamud Subir:** Conceptualization, Data curation, Formal Analysis, Funding acquisition, Investigation, Methodology, Project administration, Resources, Supervision, Visualization, Writing – original draft, Writing – review & editing.

Declaration of competing interest

The authors declare the following financial interests/personal relationships which may be considered as potential competing interests: Mahamud Subir reports financial support was provided by National Science Foundation Division of Chemistry.

Data availability

The data is presented in the manuscript and the Supplementary Material Document.

Acknowledgements

This material is based upon work supported by the National Science Foundation under Grant No. 1808468.

Appendix A. Supplementary data

Supplementary data to this article can be found online at https://doi.org/10.1016/j.chemosphere.2022.137075.

References

Akhtar, J., Amin, N.A.S., Shahzad, K., 2016. A review on removal of pharmaceuticals from water by adsorption. Desalination Water Treat. 57, 12842–12860.
Akiba, U., Fujihira, M., Preparation of Self-Assembled Monolayers (SAMs) on Au and Ag. Encyclopedia of Electrochemistry.
Ariga, K., Mori, T., Li, J., 2019. Langmuir nanoarchitectonics from basic to frontier. Langmuir 35, 3585–3599.
Bai, Y., Wu, F., Liu, C., Guo, J., Fu, P., Li, W., Xing, B., 2008. Interaction between carbamazepine and humic substances: a fluorescence spectroscopy study. Environ. Toxicol. Chem. 27, 95–102.
Bai, X.L., Lutz, A., Carroll, R., Keteles, K., Dahlin, K., Murphy, M., Nguyen, D., 2018. Occurrence, distribution, and seasonality of emerging contaminants in urban watersheds. Chemosphere 200, 133–142.
Bani-Yaseen, A.D., Al-Jaber, A.S., Ali, H.M., 2019. Probing the solute-solvent interaction of an azo-bonded prodrug in neat and binary media: combined experimental and computational study. Sci. Rep. 9, 3023.
Barnes, K.K., Kolpin, D.W., Furlong, E.T., Zaugg, S.D., Meyer, M.T., Barber, L.B., 2008. A national reconnaissance of pharmaceuticals and other organic wastewater contaminants in the United States - I) Groundwater. Sci. Total Environ. 402, 192–200.
Bhatnagar, A., Sillanpaa, M., 2017. Removal of natural organic matter (NOM) and its constituents from water by adsorption - a review. Chemosphere 166, 497–510.
Cabaleiro-Lago, E.M., Rodríguez-Otero, J., 2018. On the nature of σ–σ, σ–π, and π–π stacking in extended systems. ACS Omega 3, 9348–9359.
Caruso, F., Rodda, E., Furlong, D.N., 1996. Orientational aspects of antibody immobilization and immunological activity on quartz crystal microbalance electrodes. J. Colloid Interface Sci. 178, 104–115.
Casassas, E., Fonrodona, G., de Juan, A., 1992. Solvatochromic parameters for binary mixtures and a correlation with equilibrium constants. Part I. Dioxane-water mixtures. J. Solut. Chem. 21, 147–162.
Chaki, N.K., Vijayamohanan, K., 2002. Self-assembled monolayers as a tunable platform for biosensor applications. Biosens. Bioelectron. 17, 1–12.
Chase, H.M., Psciuk, B.T., Strick, B.L., Thomson, R.J., Batista, V.S., Geiger, F.M., 2015. Beyond local group modes in vibrational sum frequency generation. J. Phys. Chem. A 119, 3407–3414.
Chaudhari, A., Naganathappa, M., Shinde, M., Kumbharkhane, A., 2011. Theoretical investigation of molecular interactions in dioxane and water using hydrogen bonding model and density functional method. Int. J. Quant. Chem. 111, 2972–2979.
Chaukura, N., Ndlangamandla, N.G., Moyo, W., Msagati, T.A.M., Mamba, B.B., Nkambule, T.T.I., 2018. Natural organic matter in aquatic systems - a South African perspective. WaterSA 44, 624–635.
Dalla Pozza, G., Deardorff, D., Subir, M., 2022. Emerging environmental contaminants at the air/aqueous and biological soft interfaces. Environ. Sci.: Adv. 1, 430–437.
de Jesus, A.J., Yin, H., 2017. 5.14 - supramolecular membrane chemistry. In: Atwood, J.L. (Ed.), Comprehensive Supramolecular Chemistry II. Elsevier, Oxford, pp. 311–328.
Dougherty, D.A., 2013. The cation-π interaction. Acc. Chem. Res. 46, 885–893.
Easley, A.D., Ma, T., Eneh, C.I., Yun, J., Thakur, R.M., Lutkenhaus, J.L., 2022. A practical guide to quartz crystal microbalance with dissipation monitoring of thin polymer films. J. Polym. Sci. 60, 1090–1107.
Fuentes, C., Chávez, C., Quevedo, A., Trejo-Alonso, J., Fuentes, S., 2020. Modeling of artificial groundwater recharge by wells: a model stratified porous medium. Mathematics 8, 1764.
Fung, Y., Wong, Y., 2001. Self-assembled monolayers as the coating in a quartz piezoelectric crystal immunosensor to detect Salmonella in aqueous solution. Anal. Chem. 73, 5302–5309.
Halling-Sørensen, B., Nors Nielsen, S., Lanzky, P.F., Ingerslev, F., Holten Lützhøft, H.C., Jørgensen, S.E., 1998. Occurrence, fate and effects of pharmaceutical substances in the environment- A review. Chemosphere 36, 357–393.
Hanwell, M.D., Curtis, D.E., Lonie, D.C., Vandermeersch, T., Zurek, E., Hutchison, G.R., 2012. Avogadro: an advanced semantic chemical editor, visualization, and analysis platform. J. Cheminf. 4, 17.
Ho, J., Psciuk, B.T., Chase, H.M., Rudshteyn, B., Upshur, M.A., Fu, L., Thomson, R.J., Wang, H.-F., Geiger, F.M., Batista, V.S., 2016. Sum frequency generation spectroscopy and molecular dynamics simulations reveal a rotationally fluid adsorption state of α-pinene on silica. J. Phys. Chem. C 120, 12578–12589.
Hosseinpour, S., Schwind, M., Kasemo, B., Leygraf, C., Johnson, C.M., 2012. Integration of quartz crystal microbalance with vibrational sum frequency spectroscopy–quantification of the initial oxidation of alkanethiol-covered copper. J. Phys. Chem. C 116, 24549–24557.
Johnson, C.M., Baldelli, S., 2014. Vibrational sum frequency spectroscopy studies of the influence of solutes and phospholipids at vapor/water interfaces relevant to biological and environmental systems. Chem. Rev. 114, 8416–8446.
Jubb, A.M., Hua, W., Allen, H.C., 2012. Environmental chemistry at vapor/water interfaces: insights from vibrational sum frequency generation spectroscopy. Annu. Rev. Phys. Chem. 63, 107–130.
Karpovich, D.S., Blanchard, G.J., 1994. Direct measurement of the adsorption kinetics of alkanethiolate self-assembled monolayers on a microcrystalline gold surface. Langmuir 10, 3315–3322.
Karpovich, D.S., Blanchard, G.J., 1995. An undergraduate laboratory experiment for the direct measurement of monolayer-formation kinetics. J. Chem. Educ. 72, 466.
Keiluweit, M., Kleber, M., 2009. Molecular-level interactions in soils and sediments: the role of aromatic π-systems. Environ. Sci. Technol. 43, 3421–3429.
Klavins, M., Purmalis, O., 2010. Humic substances as surfactants. Environ. Chem. Lett. 8, 349–354.
Lapworth, D.J., Baran, N., Stuart, M.E., Ward, R.S., 2012. Emerging organic contaminants in groundwater: a review of sources, fate and occurrence. Environ. Pollut. 163, 287–303.
Love, J.C., Estroff, L.A., Kriebel, J.K., Nuzzo, R.G., Whitesides, G.M., 2005. Self-assembled monolayers of thiolates on metals as a form of nanotechnology. Chem. Rev. 105, 1103–1170.
McCaffrey, D.L., Nguyen, S.C., Cox, S.J., Weller, H., Alivisatos, A.P., Geissler, P.L., Saykally, R.J., 2017. Mechanism of ion adsorption to aqueous interfaces: graphene/water vs. air/water. Proc. Natl. Acad. Sci. USA 114, 13369–13373.
Molčanov, K., Kojić-Prodić, B., 2019. Towards understanding π-stacking interactions between non-aromatic rings. IUCrJ 6, 156–166.
Nagaoka, T., Chen, Z., Okuno, H., Nakayama, M., Ogura, K., 1999. Self-assembled monolayer-based electrodes for selective determination of Cu2+ and Ag+ ions with antifouling activity against protein adsorption. Anal. Sci. 15, 857–862.
Nunes, N., Elvas-Leitão, R., Martins, F., 2014. UV–Vis spectroscopic study of preferential solvation and intermolecular interactions in methanol/1-propanol/acetonitrile by means of solvatochromic probes. Spectrochim. Acta A-M. 124, 470–479.
O'Sullivan, C.K., Guilbault, G.G., 1999. Commercial quartz crystal microbalances - theory and applications. Biosens. Bioelectron. 14, 663–670.
2018. Operation and Service Manual QCM200 Quartz Crystal Microbalance. Stanford Research Systems.
Osenbrück, K., Gläser, H.-R., Knöller, K., Weise, S.M., Möder, M., Wennrich, R., Schirmer, M., Reinstorf, F., Busch, W., Strauch, G., 2007. Sources and transport of selected organic micropollutants in urban groundwater underlying the city of Halle (Saale), Germany. Water Res. 41, 3259–3270.
Rao, Y., Subir, M., McArthur, E.A., Turro, N.J., Eisenthal, K.B., 2009. Organic ions at the air/water interface. Chem. Phys. Lett. 477, 241–244.
Roshani, M.M., Rostaminikoo, E., Joonaki, E., Mirzaalian Dastjerdi, A., Najafi, B., Taghikhani, V., Hassanpouryouzband, A., 2022. Applications of the quartz crystal microbalance in energy and environmental sciences: from flow assurance to nanotechnology. Fuel 313, 122998.
Ruiz, S.H., Wickramasekara, S., Abrell, L., Gao, X., Chefetz, B., Chorover, J., 2013. Complexation of trace organic contaminants with fractionated dissolved organic matter: implications for mass spectrometric quantification. Chemosphere 91, 344–350.
Schwartz, D.K., 2001. Mechanisms and kinetics of self-assembled monolayer formation. Annu. Rev. Phys. Chem. 52, 107–137.
Spain, A., Isbell, R., Probert, M., 1983. Soil organic matter. Soils: Aust. Viewp. 551–563.
Stuart, M., Manamsa, K., Talbot, J., Crane, E., 2011. Emerging Contaminants in Groundwater.
Subir, M., Rao, Y., 2021. Environmental Interfacial Spectroscopy. American Chemical Society.
Tijani, J.O., Fatoba, O.O., Babajide, O.O., Petrik, L.F., 2016. Pharmaceuticals, endocrine disruptors, personal care products, nanomaterials and perfluorinated pollutants: a review. Environ. Chem. Lett. 14, 27–49.
Tonda-Turo, C., Carmagnola, I., Ciardelli, G., 2018. Quartz crystal microbalance with dissipation monitoring: a powerful method to predict the in vivo behavior of bioengineered surfaces. Front. Bioeng. Biotechnol. 6.
Tsou, L.K., Tatko, C.D., Waters, M.L., 2002. Simple Cation−π interaction between a phenyl ring and a protonated amine stabilizes an α-helix in water. J. Am. Chem. Soc. 124, 14917–14921.
van Oss, C.J., Giese, R.F., Docoslis, A., 2005. Hyperhydrophobicity of the water-air interface. J. Dispersion Sci. Technol. 26, 585–590.
Vashist, S.K., Vashist, P., 2011. Recent advances in quartz crystal microbalance-based sensors. J. Sens. 571405. 2011.
Vogt, B.D., Lin, E.K., Wu, W.-l., White, C.C., 2004. Effect of film thickness on the validity of the Sauerbrey equation for hydrated polyelectrolyte films. J. Phys. Chem. B 108, 12685–12690.
Wang, B., Liu, C., Chen, Y., Dong, F., Chen, S., Zhang, D., Zhu, J., 2018. Structural characteristics, analytical techniques and interactions with organic contaminants of dissolved organic matter derived from crop straw: a critical review. RSC Adv. 8, 36927–36938.
Wang, M., Shi, H., Shao, S., Lu, K., Wang, H., Yang, Y., Gong, Z., Zuo, Y., Gao, S., 2022a. Montmorillonite promoted photodegradation of amlodipine in natural water via formation of surface complexes. Chemosphere 286, 131641.
Wang, Y., Liu, J., Liem-Nguyen, V., Tian, S., Zhang, S., Wang, D., Jiang, T., 2022b. Binding strength of mercury (II) to different dissolved organic matter: the roles of DOM properties and sources. Sci. Total Environ. 807, 150979.
Wilkinson, J., Hooda, P.S., Barker, J., Barton, S., Swinden, J., 2017. Occurrence, fate and transformation of emerging contaminants in water: an overarching review of the field. Environ. Pollut. 231, 954–970.
Williams, T.A., Lee, J., Diemler, C.A., Subir, M., 2016. Magnetic vs. non-magnetic colloids – a comparative adsorption study to quantify the effect of dye-induced aggregation on the binding affinity of an organic dye. J. Colloid Interface Sci. 481, 20–27.

Williams, T., Walsh, C., Murray, K., Subir, M., 2020. Interactions of emerging contaminants with model colloidal microplastics, C60 fullerene, and natural organic matter – effect of surface functional group and adsorbate properties. Environ. Sci.: Process. Impacts 22, 1190–1200.
Wu, F.C., Bai, Y.C., Mu, Y.S., Pan, B., Xing, B.S., Lin, Y., 2013. Fluorescence quenching of fulvic acids by fullerene in water. Environ. Pollut. 172, 100–107.
Yang, Y., Chen, Y., Zhao, Y., Shi, W., Ma, F., Li, Y., 2019. Under different solvents excited-state intramolecular proton transfer mechanism and solvatochromic effect of 2-(2-hydroxyphenyl) benzothiazole molecule. J. Lumin. 206, 326–334.
Zhang, S., Li, F., Yu, F., Jiang, X., Lee, H.-Y., Luo, J., Shrout, T.R., 2018. Recent developments in piezoelectric crystals. J. Korean Ceram. Soc. 55, 419–439.
Zhang, J.J., Mou, L., Jiang, X.Y., 2020. Surface chemistry of gold nanoparticles for health-related applications. Chem. Sci. 11, 923–936.
Zhang, D., Yang, S., Yang, C., Chen, Y., Hu, R., Xie, Y., Wang, Y., Wang, W., 2022a. New insights into the interaction between dissolved organic matter and different types of antibiotics, oxytetracycline and sulfadiazine: multi-spectroscopic methods and density functional theory calculations. Sci. Total Environ. 820, 153258.
Zhang, H., Cheng, H., Wang, Y., Duan, Z., Cui, W., Shi, Y., Qin, L., 2022b. Influence of functional group modification on the toxicity of nanoplastics. Front. Mar. Sci. 8.